

Using HIRS Observations to Construct Long-Term Global Temperature and Water Vapor Profile Time Series

Lei Shi and John J. Bates

*National Climatic Data Center, National Oceanic and Atmospheric Administration
Asheville, North Carolina, USA*

Introduction

The HIRS instrument has been flown onboard the NOAA polar satellite series since 1978. The long-term measurement provides a valuable source for assessing global climatic change in the past decades. In this study, twelve channels in the longwave spectrum regime (channels 1-12) of the HIRS instrument are used to derive long-term temperature and water vapor in the troposphere.

Previous work has generated a time series of cloud-cleared dataset at the HIRS original swath resolution (Jackson and Bates, 2001). Using an inter-satellite calibrated version of the dataset, Bates and Jackson (2001) and Bates et al. (2001) examined the variability of upper tropospheric humidity. These studies showed that while the inter-annual variability of spatial fields was dominated by the major El Niño events, the upper tropospheric humidity exhibited more prominent seasonal variation.

The current study uses a neural network technique to derive temperature and water vapor profiles at different levels of the atmosphere. A neural network algorithm was discussed in Shi (2001), in which neural networks were applied to regional direct acquisition and global recorded NOAA-15 Advanced Microwave Sounding Unit measurements. The study showed significantly smaller root mean square values from neural network retrieval compared to a linear regression method.

Neural network retrieval

Backpropagation neural networks similar to those applied by Shi (2001) are used in developing the retrieval scheme. The neural network training dataset is based on a diverse sample of profiles simulated by the European Center for Medium-Range Weather Forecasts (ECMWF) system (Chevallier, 2001). The model profiles are generated by the ERA-40 assimilation system with the 3-dimensional variational scheme described by Courtier et al. (1998). The profiles are selected from the first and the 15th of each month between January 1992 and December 1993. The profiles are divided into seven groups differing by the total precipitable water vapor content of the profiles. About the same number of samples is extracted from each group, except for the group with the lowest precipitable water vapor content (0 to 0.5 kg.m⁻²). For this group, twice as many profiles are extracted in consideration of the higher temperature variability from all types of

situations. The corresponding HIRS channel brightness temperatures are simulated by a radiative transfer model, RTTOV-8. The RTTOV is a broadband model in which the integration over the channel response is simulated directly. A description of the RTTOV can be found in Saunders et al. (1999). The RTTOV was one of the participating models in an intercomparison of HIRS and AMSU channel radiance computation (Garand et al., 2001). Among the seven selected HIRS channels (channels 2, 5, 9, 10, 11, 12, and 15) examined, the standard deviations of RTTOV simulated radiances are within 0.25 K for the five non-water vapor channels, and within 0.55 K for the two water vapor channels.

The HIRS channels 1-8 are located in the CO₂ absorption band which is temperature sensitive. The measurement assumes constant CO₂ concentration in the atmosphere. However, through the 25 years of the HIRS data series, the CO₂ concentration increased from 330 ppmv to more than 370 ppmv. To quantify the effect of CO₂ increase on the HIRS channel measurements, we use RTTOV-8 to compute the channel brightness temperatures of the sample set of the atmospheric profiles at CO₂ values of 330 and 370 ppmv. The differences in channel brightness temperatures are displayed in Fig. 1. The figure shows that the CO₂ increase has a significant impact on many of the sounding channels, most remarkably at channels 4-7, which sense the atmospheric temperature from 900 to 150 hPa. When no change is made in the atmospheric profiles, the increase of CO₂ alone from 330 to 370 ppmv can cause about 1 K decrease of brightness temperatures in channels 4, 5, and 6. The same amount of CO₂ change can increase the brightness temperature in channels 1 and 2 by approximately 0.4 K. To account for the impact from the CO₂ increase, the HIRS channel radiances for the neural network training datasets are computed by RTTOV-8 at a CO₂ increment of 10 ppmv. The simulated HIRS brightness temperatures are collocated with the input profiles and placed in the training dataset.

A five-layer backpropagation network, with one input layer, three hidden layers, and one output layer, is applied for the retrieval. Different transfer functions are examined for temperature and water vapor retrieval performance. The best performance is obtained by a selection of the hyperbolic tangent, Gaussian, and logistic functions. The definitions of these functions are, respectively,

$$f(x) = \tanh(x), \tag{1}$$

$$f(x) = \exp(-x^2), \text{ and} \tag{2}$$

$$f(x) = \frac{1}{1 + \exp(-x)}. \tag{3}$$

The numbers of neurons in the hidden layers are adjusted to optimize the performance. The input set includes the twelve HIRS longwave channels and the CO₂ concentration. The retrieval temperatures are obtained at 18 pressure levels from 1005 hPa to 50 hPa, and the water vapor mixing ratios are obtained at 13 levels from 1005 hPa to 300 hPa. Because the neural network training dataset requires values at each pressure level, the training profiles with the surface pressure value less than 975 hPa are excluded. This builds a total of 9978 collocated patterns.

Among these patterns, 20% (1955 patterns) are randomly extracted to construct a testing set, and another 20% are randomly extracted and set aside as a validation set for later statistical studies. As a result, there are 5988 patterns remaining and they are kept in the learning set. A backpropagation network is trained by “supervised learning”. The network is presented with a series of pattern pairs, each consisting of an input pattern and an output pattern, in random order until predetermined convergence criteria are met. At this time the network presents the input elements in the testing set and retrieves the output elements. Then the retrieved output elements are compared with the output elements in the testing set, and the averaged root mean square error (RMSE) of all the output elements is computed. The network parameters are saved if the averaged RMSE is less than that computed previously. This process is repeated until no improvement is found for a specified number of test trials.

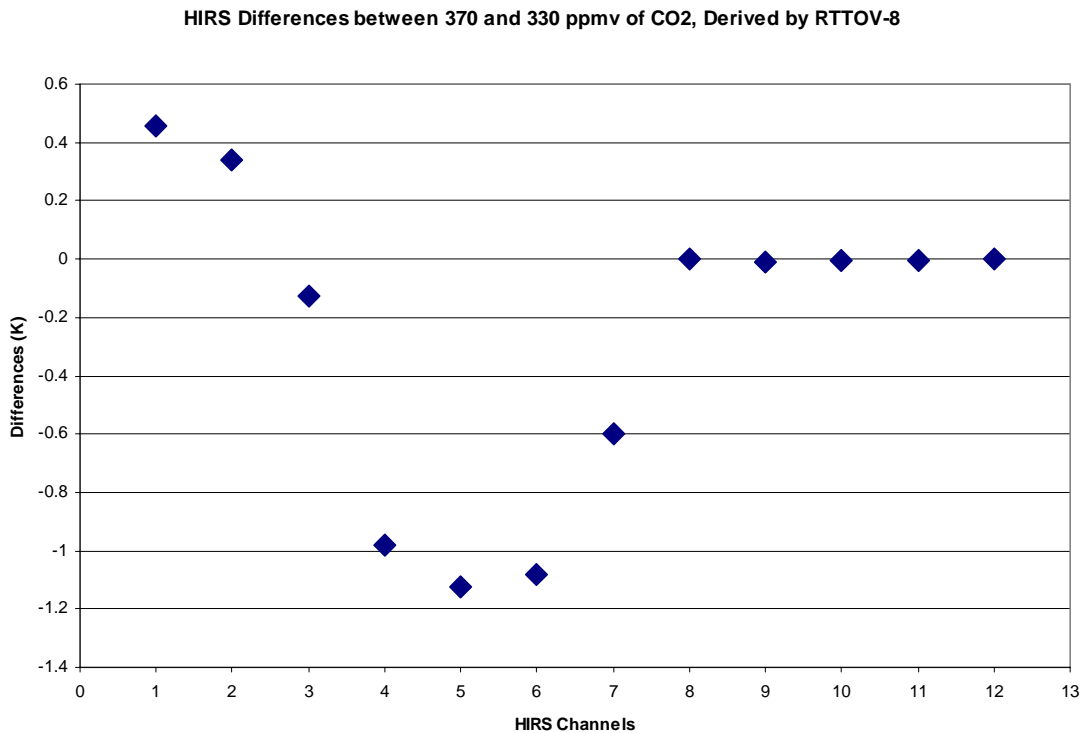


Fig. 1. Differences in HIRS channel brightness temperatures when carbon dioxide increases from 330 to 370 ppmv.

For both temperature and water vapor retrievals, one neural network function is developed for each of the satellites from TIROS-N, NOAA-6, to NOAA-14 based on the individual HIRS simulation of RTTOV-8. The RMSE of each function is computed using the output pattern in the validation data set as truth data. The RMSEs for different satellites are slightly different. In general, for temperature retrieval, the RMSEs are about 2°C at near-surface levels, 1.1-1.2°C in

the mid-troposphere, and about 2°C around the tropopause and in the lower stratosphere. For water vapor, the RMSEs are about 2 g/kg at the surface level. They steadily decrease to around 1 g/kg at 700 hPa and less than 0.5 g/kg above 500 hPa.

Temperature and water vapor time series

For each satellite, the temperature and water vapor profiles are computed using the neural network retrieval functions at each of the clear-sky pixels. The values are then averaged at each 2.5x2.5 latitude/longitude grids at every 3 hour interval. An eastern Pacific area bounded by 20°S-20°N and 160°W-100°W has been selected to facilitate inter-satellite calibration. As an example of the temperature variability, Fig. 2 shows a time series of monthly mean temperature for 0-3 UTC at 479 hPa for the tropical zone between 30°S and 30°N. Each filled circle represents the monthly mean, and each square is a 13-point running average. The time series starts at January 1980 and extends through December 2004. For the tropical region, the monthly mean values depict the annual cycle of the temperature change. The 13-point running averages smooth out the annual variation and reveal the variation in a longer time scale. The smoothed plots capture the major events in the time series. For example, the plots show the increased temperatures in the 1986-1987 and 1997 El Niño episodes. The La Niña events in 1988-1989 and in 1998-1999 are also shown as decreased temperatures. There is a trend of increasing temperature though the 25 year time series.

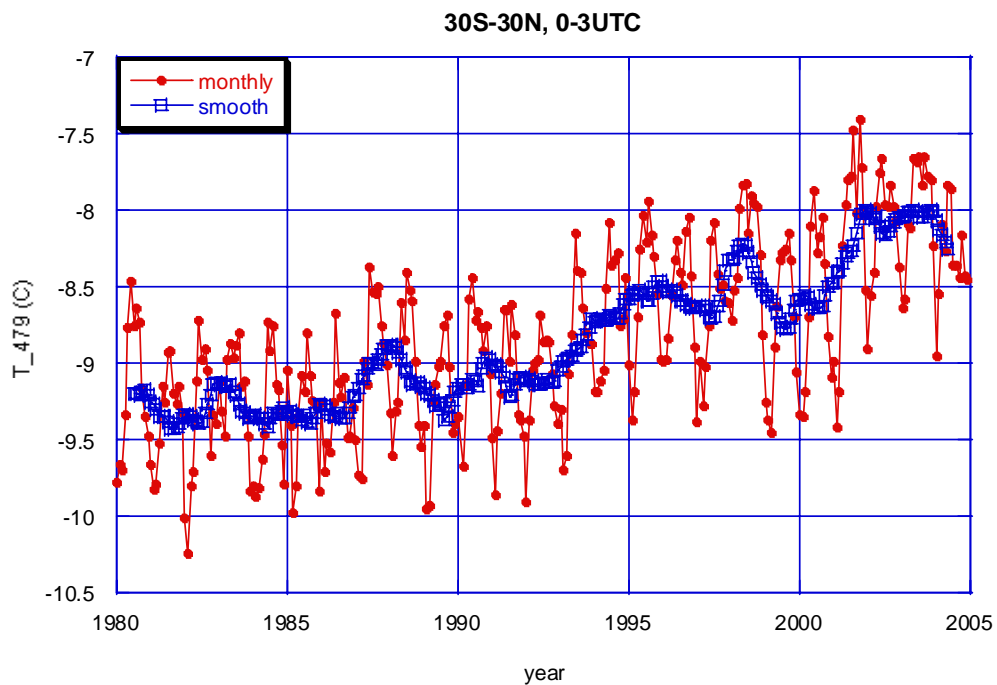


Fig. 2. Plots of monthly mean temperature (filled dots) for 0-3 UTC at 479 hPa for the latitude zone between 30S and 30N. The 13-point averages are plotted as squares.

The tropical monthly mean mixing ratio time series for 0-3 UTC at 397 hPa is plotted in Fig. 3. The major El Niño and La Niña events are also reflected in the time series. Comparing the mixing ratio with the time series of sea surface temperature (SST) anomalies in the equatorial Pacific regions as shown in Bates et al. (2001), there appears to be an association of peak values between the two time series. The peak values in the mixing ratio time series in 1982-1983 and 1997-1998 are observed during the extreme El Niño events in the SST anomaly time series.

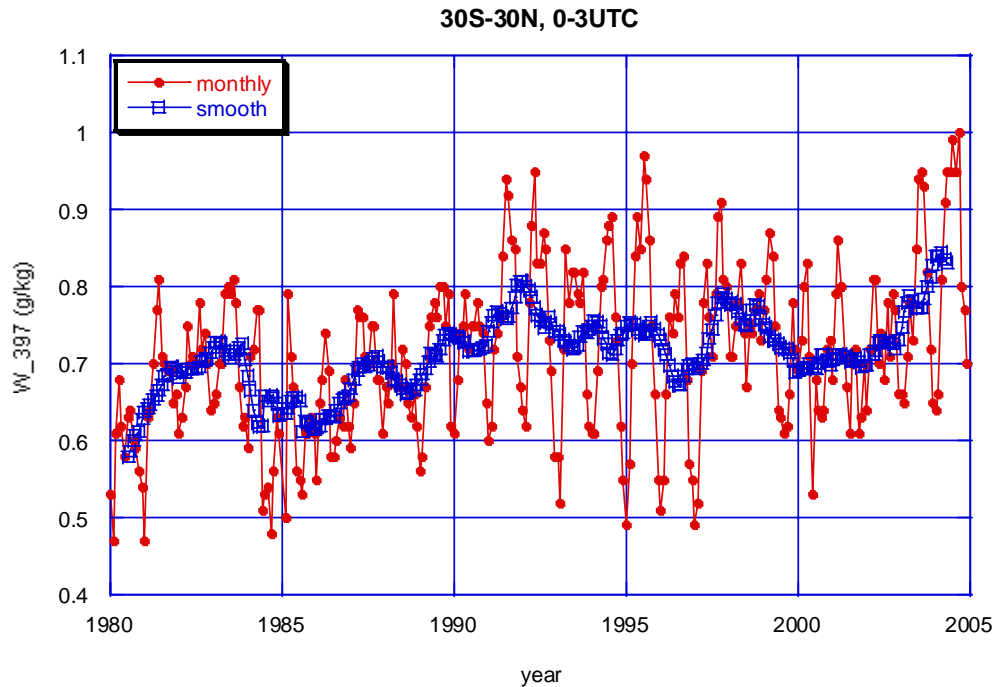


Fig. 3. Same as Fig. 2 except for water vapor (g/kg) at 397 hPa.

Summary

A retrieval scheme based on neural network technique is developed to derive temperature and vapor profiles. The training dataset is constructed with a diverse sample of atmospheric profiles from ECMWF reanalysis data and simulated HIRS brightness temperatures by the latest version of the broad band radiative transfer model, RTTOV-8. Considering that the majority of HIRS channels are located in the carbon dioxide absorption band, the impact of carbon dioxide increase on the long-term HIRS measurement is examined in this study. Based on radiative transfer model simulation, it is found that when carbon dioxide concentration increases from 330 ppmv to 370 ppmv, the impact to the HIRS channel measurement can be as large as 1 K. The largest impact is on HIRS channels 4, 5, and 6. To account for the effect from carbon dioxide increase, the variation of carbon dioxide concentration is included as one of the input variables in the retrieval scheme.

A 25-year time series of temperature and water vapor at selected latitude zones is constructed. In addition to monthly mean values which display annual cycles of temperature and water vapor, a 13-point moving average plot shows variations in a longer time scale. The time series for the tropical zone captures the major events such as El Niño and La Niña episodes. The water vapor shows more inter-annual variability than the temperature time series. Both temperature and water vapor plots show an increasing trend in the 25-year time series. The significance of the temperature and water vapor increase needs further evaluation. In order to obtain an accurate measure of temperature and water vapor trend, a good inter-satellite calibration scheme is required. The next steps of the study will include applying a better inter-satellite calibration algorithm and validation of the retrievals using other independent data sources.

Acknowledgment. Darren Jackson provided the HIRS clear-sky data from 1978 to 2001 and codes for processing data from 2002 to 2004.

References

- Bates, J. J. and Jackson, D.L. 2001. Trends in upper-tropospheric humidity. *Geophys. Res. Letters*, **28**, 1695-1698.
- Bates, J. J., Jackson, D.L., Breon, F.-M. and Bergen, Z.D. 2001. Variability of tropical upper tropospheric humidity 1979-1998. *J. Geophys. Res.*, **106**, 32371-32281.
- Chevallier, F. 2001. Sampled databases of 60-level atmospheric profiles from the ECMWF analyses. Research Report No. 4, EUMETSAT/ECMWF SAF programme.
- Courtier, P., Anderson, E., Heckley, W., Pailleux, J., Vasiljevic, D., Hamrud, M., Hollingsworth, A., Rabier, F., and Fisher, M. 1998. The ECMWF implementation of three dimensional variational assimilation (3D-Var). Part I: formation. *Q. J. Roy. Meteor. Soc.*, **124**, 1783-1808.
- Garand, L., Turner, D.S., Larocque, M., Bates, J., Boukabara, S., Brunel, P., Chevallier, F., Deblonde, G., Engelen, R., Hollingshead, M., Jackson, D., Jedlovec, G., Joiner, J., Kleespies, T., McKague, D.S., MaMillin, L., Moncet, J.-L., Pardo, J.R., Rayer, P.L., Salathe, E., Saunders, R., Scott, N.A., Van Delst, P. and Woolf, H. 2001. Radiance and Jacobian intercomparison of radiative transfer models applied to HIRS and AMSU channels. *J. Geophys. Res.*, **106**, 24017-24031.
- Jackson, D. L. and Bates, J. J. 2001. Climate analysis with the 21-yr HIRS Pathfinder Radiance clear-sky data set. Proc. 11th Conference on Satellite Meteorology and Oceanography, October 15-18, Madison, WI, 138-140.
- Saunders R.W., Matricardi M. and Brunel, P. 1999. An improved fast radiative transfer model for assimilation of satellite radiance observations, *Q. J. Royal Meteorol. Soc.*, **125**, 1407-1426.
- Shi, L., 2001. Retrieval of atmospheric temperature profiles from AMSU-A measurement using a neural network approach. *J. Atmos. Ocean. Tech.*, **18**, 340-347.